



City Research Online

City, University of London Institutional Repository

Citation: Khan, S. ORCID: 0000-0001-5589-6914 and Abdullah, F. (1991). Computer Aided Design of Process Tomography Capacitance Electrode System for Flow Imaging. In: Grattan, K. T. V. ORCID: 0000-0003-2250-3832 (Ed.), *Sensors, Technology, Systems and Applications*. (pp. 209-214). Florida, USA: CRC Press. ISBN 9780750301572

This is the accepted version of the paper.

This version of the publication may differ from the final published version.

Permanent repository link: <https://openaccess.city.ac.uk/id/eprint/23730/>

Link to published version:

Copyright and reuse: City Research Online aims to make research outputs of City, University of London available to a wider audience. Copyright and Moral Rights remain with the author(s) and/or copyright holders. URLs from City Research Online may be freely distributed and linked to.

City Research Online:

<http://openaccess.city.ac.uk/>

publications@city.ac.uk

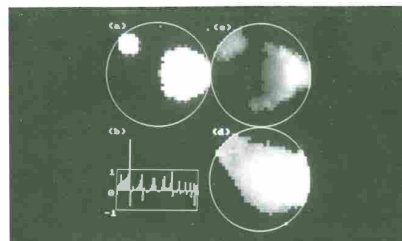


Fig.5. (a) Same flow phase distribution model as that shown in Fig.4a; (b) capacitance data λ_{ij} of flow model (a), calculated for a sensor with $R_2-R_1=20\text{mm}$ and with other sensor parameters being the same as those stated in Fig.4b; (c) same as in Fig.4c; (d) same as in Fig.4d.

exhibit much higher degree of non-linearity. Consequently, the reconstructed image has poorer fidelity (process P4 is again involved). Fig.5d gives the image reconstructed using the binary sensitivity information mentioned above. It has been found that, for gas/oil flow, images reconstructed using primary sensors with pipe-liner thickness $R_2-R_1=5\text{mm}$ and 10mm are all less satisfactory than those reconstructed using a primary sensor with $R_2-R_1=15\text{mm}$ (other sensor parameters remain unchanged). Therefore, a sensor with pipe-liner thickness $R_2-R_1=15\text{mm}$ is the optimal choice. Note that, for other two-component flows, such as an oil/water flow, this design is not necessarily the optimal one and a new design has to be performed. Other aspects on sensor design can be found elsewhere (Khan and Abdullah 1991).

4. CONCLUSIONS

In this paper, a software environment has been demonstrated to be capable of providing useful tools for the development of new image reconstruction algorithms and the design of optimal sensors for capacitive tomography.

ACKNOWLEDGMENT

The authors acknowledge the SERC and DTI for supporting this work through a grant under the LINK scheme and thank the industrial partners of the project, the Schlumberger Cambridge Research and the Schlumberger Industries.

REFERENCES

- Huang S M, Xie C G, Thorn R, Snowden D and Beck M S 1991 (submitted)
- Hughes T J R 1987 *The finite element method — linear static and dynamic finite element analysis* (London: Prentice-Hall International)
- S Khan and F Abdullah 1991 (submitted)
- Xie C G, Plaskowski A and Beck M S 1989 *IEE Proc. Pt.A* 136 173–91

Computer aided design of process tomography capacitance electrode system for flow imaging

S H Khan F Abdullah

Measurement and Instrumentation Centre, Department of EE and Information Engineering, City University, Northampton Square, London EC1V 0HB, UK

ABSTRACT: This paper involves various aspects and results for the computer aided design of capacitance electrode systems used for imaging and measurement of two-phase flows. Various 2D finite element models of a 12-electrode system have been investigated to show the effects of a wide range of design parameters on system performance. Recommendations have been made for the selection of some of these parameters which could give desirable system performance.

1. INTRODUCTION

Although computer aided tomography is quite established in medical practice for imaging human internal organs, application of similar techniques but using capacitance electrode systems for flow imaging in industrial processes is comparatively new. This technique, in which a number of capacitance electrodes are mounted circumferentially around the flow pipe and interrogated in turn by electronic control is based on changes in capacitance values between electrodes due to the change in permittivities of flow components. Beck *et al.* (1986) proposed this for imaging multiphase flows and the idea has been further developed at UMIST by Huang *et al.* (1989). It has been found that such multielectrode systems have considerable potential to be used in process industry, especially the oil industry. Hence, the term 'process tomography' has been introduced. Unlike other techniques capacitance technique has the advantage of being cheap, fast, noninvasive, nonintrusive and simple to construct.

The performance of a multielectrode capacitance system depends on its geometric parameters. The electric field distribution inside the flow pipe is non-uniform and changes with system parameters. This results in a non-uniform sensitivity distribution over the pipe cross-section which, for consistent and effective functioning of the system is undesirable. CAD of electrode systems which involves accurate field modelling, capacitance calculations, etc. is, therefore important to optimize system parameters and achieve desirable performance. At present there are a few published works on CAD of such systems. Theoretical aspects and finite element modelling of an 8-electrode system has been discussed by Xie *et al.* (1989). Their recent work involves design optimization of a 2-electrode system for concentration measurement of two-phase flows.

In this paper, particular emphasis is given on critical aspects of CAD and performance analysis by finite element method (FEM) of a 12-electrode capacitance system for two-phase flows. A large number of models have been

investigated to evaluate, quantitatively variations in field and so the sensitivity distributions inside the flow pipe for a wide range of system parameters.

2. WORKING PRINCIPLE AND GEOMETRIC PARAMETERS OF A MULTIELECTRODE CAPACITANCE SYSTEM

Figure 1 shows the cross section of a 12-electrode system which consists of 12 capacitance electrodes, mounted symmetrically on the outer surface of the insulating wall of a special section of the pipeline. The radial screens in between electrodes reduce high capacitance between neighbouring electrodes and force the electric field in towards the central region. The earthed outer screen with inner radius R_3 acts as a shield to make the whole system stray immune. Inner radius, R_1 of the pipe wall is fixed but its outer radius, R_2 and hence thickness, $\delta_1=R_2-R_1$ can vary. The empty space between pipe wall outer surface and outer screen is filled with dielectric filling material to insulate electrodes from the screen.

For data acquisition one of the electrodes, say 1 (active electrode) is given a constant potential (the rest - kept at zero potential) and another electrode, say 2 is selected as 'detecting electrode' and the capacitance between 1 and 2 is measured by discharging 1 through special capacitance measuring circuitry (Huang *et al* 1989). In a similar way capacitances between rest of the electrode pairs 1-3, 1-4, 1-5, ..., 1-12 are measured which completes one data acquisition cycle. The next cycle begins with electrode 2, selected as the active electrode; the whole process of data acquisition finishes with the 11-th cycle with electrode 11 acting as the active electrode. For an N -electrode system this gives a total of $n = N(N-1)/2$ independent measurements.

The electric field between electrodes and so the above capacitance measurements change with dielectric distributions inside the pipeline. For any selected pair of electrodes a narrow region of positive sensitivity can be found within which an unit dielectric increase leads to an increase in their capacitance measurements. The presence of a dielectric material inside this region can thus be detected from measured capacitance values. These regions for all selected pair of electrodes create, for a given geometry total positive sensing area of the electrode system over pipeline cross-section. As shown by Huang *et al* (1989), by exploiting the functional relationship between measured capacitance values, dielectric distribution and sensitivity distribution function one can solve the inverse problem of determining the flow component distribution over pipe cross-section using measured capacitance values. A dedicated image reconstruction algorithm can be used to solve this problem and see the flow component distribution inside the pipeline (Xie *et al* 1989).

The quality of the reconstructed image depends on the uniformity of

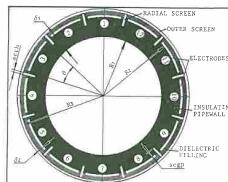


Fig. 1. Cross section of a 12-electrode capacitance system for flow imaging (not in scale)

sensitivity distribution which, as said earlier depends on following system geometric parameters shown in Figure 1: number of electrodes N , electrode angle θ , pipe wall thickness δ_1 , thickness of the space between pipe wall outer surface and outer screen $\delta_2=R_3-R_2$, radial screen thickness δ_{sch} and its penetration depth inside the pipe wall δ_{pdp} . These parameters need to be optimized to get the best system performance.

3. FINITE ELEMENT MODELLING OF 12-ELECTRODE CAPACITANCE SYSTEM

By assuming that a) fringing field effects due to finite lengths of electrodes are negligible and b) flow component distributions do not change spatially along the axial direction (at least within electrode lengths) of the pipeline (e.g. core flow, annular flow, etc.) the processes in the electrode system in Figure 1 can be simulated using the 2D finite element (FE) model, shown in Figure 2. For radially symmetrical flows electric field distribution between electrodes is symmetrical which allows only half of the model to be used. This increases accuracy of FE solutions since finer mesh can be generated for the same number of nodes.

For space-varying permittivities of flow component distributions, $\epsilon=\epsilon(x,y)$ the electric field in the electrode system can be calculated (assuming free charge distribution) by solving the following Laplace's equation in terms of electrostatic potential, $\Phi = \Phi(x,y)$

$$\nabla \cdot (\epsilon \nabla \Phi) = 0 \quad (1)$$

This equation has been solved by FEM (using Vector Fields package PE2D on a Sun SPARCstation 1) under boundary conditions shown in Figure 2 which gives potential values at nodes from which field component vectors like E , D can be calculated. As the accuracy of FE solution depends on various aspects of discretisation special care has been taken to minimise discretisation errors (with typical total number of elements - nearly 10000). Consistent mesh pattern has been maintained for different models to make valid the comparability of the results. After solving eq. (1) capacitances between electrode pairs are found by calculating the total charge on the detecting electrode (by integration using Gauss's Law).

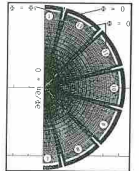


Fig. 2. Finite element model of the 12-electrode capacitance system

To analyse the effects of geometric parameters following system performance parameters have been used: a) standing mode capacitance, Co_{ij} - capacitance between electrode pair $i-j$ when the pipe is empty (relative permittivity $\epsilon = \epsilon_0$); b) absolute sensitivity of the system, $AC_{ij} = (C_{ij} - Co_{ij})/1$ where, C_{ij} - capacitance between electrode pair $i-j$ when only the k -th elementary finite element region inside the pipe (shown shaded in Figure 10) has permittivity $\epsilon = \epsilon_k$; 1 - length of electrodes; c) relative sensitivity of the system, $SI_{ij} = ((C_{ij} - Co_{ij})/Co_{ij}) \cdot (Ao/A_k)$ where, Ao is the cross-sectional area of the pipeline, A_k - area of k -th finite element region.

4. RESULTS AND DISCUSSIONS

One of the main parameters of multielectrode capacitance systems is the number of electrodes, N the selection of which could depend on the following: as shown by Xie *et al* (1989) image resolution of the system increases as the number of independent capacitance measurements, n

increases. Since $n = N(N-1)/2$ the higher the N the better is the image resolution. At the same time, as N increases the data acquisition and image reconstruction time increases which should be avoided as flow imaging system must have high performance speed due to high speed of flow components. Moreover, as N increases the electrode angle θ decreases with which increases the minimum detectable void fraction β (cross sectional area of an elongated bubble flow relative to A_0) by the system. For example, for a gap of 3 degrees between neighbouring electrodes, the angle θ for 12 and an equivalent 24-electrode systems are 25 and 10 degrees respectively. As shown in Figure 3 such a 12-electrode system should be able to detect 3 times smaller void fraction than the 24-electrode one. Moreover, capacitances C_{ij} and C_j decrease as N increases, so larger N requires more sensitive measuring circuits. Considering all these $N=12$ seems to be a reasonable trade off. However, for slower flows N could be increased (provided the availability of proper measuring electronics, etc.) to get higher resolution in flow imaging.

For a given electrode system maximum and minimum capacitances C_{max} and C_{min} depend on θ . In order to increase measurement accuracy it is desirable to minimise their ratio $K_c = C_{max}/C_{min}$. Figure 4 shows how K_c changes with θ for 8 and 12-electrode systems. This, in conjunction with what has been said earlier could be used to choose θ .

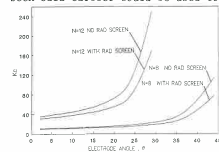


Fig. 4. Variation of K_c with electrode angle, θ

The parameter δ_2 also influences K_c . As shown in Figure 5 K_c increases as δ_2 increases which suggests that δ_2 should be taken as small as possible. Although other results show that β changes insignificantly with δ_2 , various technological factors should also be taken into account when selecting δ_2 .

Radial screens, proposed by researchers at UMIST are novel features in multielectrode systems. For obvious geometric reasons capacitances between active electrodes and their closest neighbours (C_{max}) can be much higher than those between active and farthest electrodes (C_{min}). The main purpose of radial screens is to shield the electric field from the active electrode to neighbouring ones and thus decrease K_c . This increases measurement accuracy. The shielding effects of the radial screen between electrodes 1 (active) and 12 can be seen clearly by comparing equipotential plots for the 12-electrode system in Figures 6a, b. In Figure 6a, the screen does not

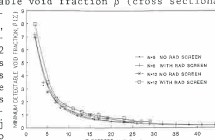


Fig. 3. Variation of minimum detectable void fraction, β , with electrode angle, θ

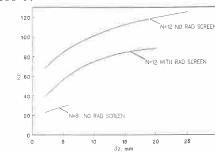


Fig. 5. Variation of K_c with $\delta_2 = R_3 - R_2$

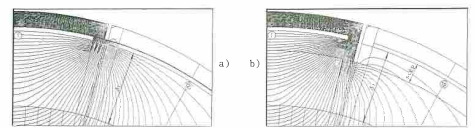


Fig. 6. Equipotential plots for the 12-electrode capacitance system showing effects of radial screens a) $scgp = 0$ b) $scgp = 5$ mm

penetrate the pipe wall ($scgp=0$) but in Figures 6b it does ($scgp=5$ mm). Quantitatively, these effects can be seen from $K_c = f(\theta)$ and $K_c = f(\delta_2)$ curves shown in Figures 4 and 5. The introduction of radial screens is thus justified. However, as shown below for a given δ_1 their effectiveness depends mostly on $scgp$ and $scsh$ which apart from shielding, affect the sensitivity distribution inside the pipe.

Standing mode capacitances between electrodes change with $scsh$ although other results show that it does not (when $scgp=const.$) virtually affect the sensitivity distributions. Figure 7 shows variations of capacitance C_{0112} between electrode pair 1 - 12 with $scsh$ for different $scgp$. It shows that these capacitances decrease as $scgp$ and $scsh$ increase which suggests that a larger $scgp$ should be avoided. Furthermore, it is evident from Figure 7 that from shielding point of view a shorter and thicker screen can be as effective as the longer and thinner one. Technologically a shorter $scgp$ is more preferable.

Figures 8 and 9 show some of the effects of δ_1 and $scgp$ on sensitivity distribution between electrode pairs 1 - 7 and 1 - 12. The sensitivities S_{17}

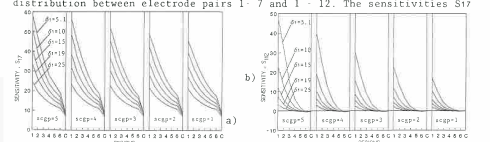


Fig. 7. Variations of C_{0112} with $scsh$ ($\delta_1=const.$); $scgp$ in mm

and S_{12} have been calculated through respective changes in capacitances due to the change in permittivity of elementary regions (one at a time from C_0 to C_N) along the radius (radial regions) and on an arc (regions on arc) close to the pipe wall (Figure 10). In Figures 8 and 9 the numbers (1, 2, 3, ...) along x-axis correspond to positions of these regions. In

Fig. 8. Variations of sensitivities a) S_{17} and b) S_{12} with region position (radial regions); δ_1 and $scgp$ in mm

and S_{12} have been calculated through respective changes in capacitances due to the change in permittivity of elementary regions (one at a time from C_0 to C_N) along the radius (radial regions) and on an arc (regions on arc) close to the pipe wall (Figure 10). In Figures 8 and 9 the numbers (1, 2, 3, ...) along x-axis correspond to positions of these regions. In

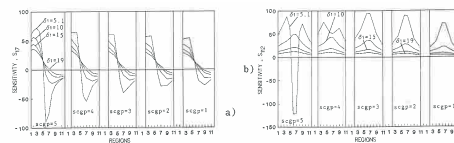


Fig. 9. Variations of sensitivities a) S_{17} and b) S_{12} with region position (regions on arc); δt and $scgp$ in mm

Figures 8a and 8b 'C's along x-axis represent the position of an elementary region at the centre of the pipe. Careful analysis of Figures 8 and 9 shows that pipe wall thickness plays an important role in sensitivity distributions - more uniform distribution could be achieved by using a thinner pipe wall. Furthermore, for a given δt an increase in $scgp$ results in more uniform sensitivity distribution. However, taking into account what has been said earlier it becomes apparent that a thinner pipe wall with shorter radial screens could well be a better option.

5. CONCLUSION

Although details of the CAD of multielectrode capacitance systems are beyond the scope of this paper some of the main features and results so far obtained have been discussed. These show the effectiveness and importance of CAD approach towards the understanding of electrode systems and their design optimization. The results of the above study have been used in the design of 12-electrode prototype systems.

6. ACKNOWLEDGEMENTS

The authors would like to express their thanks and sincere gratitude to professor M. S. Beck, Dr. C. G. Xie and Dr. S. M. Huang at UMIST for their guidance and valuable discussions at all stages of the work. The authors would also like to thank SERC for financial support.

7. REFERENCES

- Beck M S, Plaskowski A and Green R G 1986 *Proceedings of the 4th International Symposium on Flow Visualization*, 26 - 28 August 1986 (Hemisphere Publishing Corporation) pp 585 - 588
- Huang S M, Plaskowski A B, Xie C G and Beck M S 1989 *J. Phys. E, Sci. Instrum.* 22 pp 173 - 177
- Xie C G, Plaskowski A and Beck M S 1989 *IEE Proc.* 136 (4) pp 173 - 183
- Xie C G, Stott A L, Plaskowski A and Beck M S 1990 *Meas. Sci. Technol.* 1 pp 63 - 78

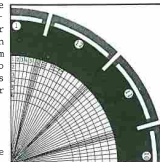


Fig. 10. FE model showing positions of elementary regions